IAI Accepts, published online ahead of print on 25 November 2013
Infect. Immun. doi:10.1128/IAI.00855-13
Copyright © 2013, American Society for Microbiology. All Rights Reserved.

IAI Accepts published online ahead of print

The Impact of Surfactant Protein D, Interleukin-5, and Eosinophilia on Cryptococcosis

Stephanie M. Holmer,[a] Kathy S. Evans,[b] Yohannes G. Asfaw,[d] Divey Saini,[e] Wiley A. Schell,[b] Julie G. Ledford,[a,b] Richard Frothingham,[b,e] Jo Rae Wright,[†] Gregory D. Sempowski,[b,c,e] and John R. Perfect [b*]

Departments of Cell Biology,[a] Medicine,[b] and Pathology,[c] Division of Laboratory Animal Resources,[d] and Duke Human Vaccine Institute,[e] Duke University Medical Center, Durham, North Carolina, USA.

[*]**Corresponding author:** John R. Perfect, M.D., Duke University Medical Center, john.perfect@duke.edu

[†]Deceased.

Running title: SP-D, IL-5, Eosinophilia and Cryptococcosis

Keywords: *Cryptococcus neoformans*, Surfactant Protein-D, eosinophils, interleukin-5, pulmonary immunology

Downloaded from http://iai.asm.org/ on November 28, 2020 by guest

IAI Accepts published online ahead of print

Abstract

Cryptococcus neoformans is an opportunistic fungal pathogen that initiates infection following inhalation. As a result, the pulmonary immune response provides a first line of defense against *C. neoformans*. Surfactant protein D (SP-D) is an important regulator of pulmonary immune responses and is typically host-protective against bacterial and viral respiratory infections. However, SP-D is not protective against *C. neoformans*. This is evidenced by previous work from our laboratory demonstrating that SP-D deficient mice infected with *C. neoformans* have a lower fungal burden and live longer, compared to wild-type (WT) control animals. We hypothesized that SP-D alters susceptibility to *C. neoformans* by dysregulating the innate pulmonary immune response following infection. Thus inflammatory cells and cytokines were compared in the bronchoalveolar lavage fluid from WT and SP-D$^{-/-}$ mice after *C. neoformans* infection. Post-infection, mice lacking SP-D have reduced eosinophil infiltration and IL-5 in lung lavage fluid. To further explore the interplay of SP-D, eosinophils, and IL-5, mice expressing altered levels of eosinophils and/or IL-5 were infected with *C. neoformans* to assess the role of these innate immune mediators. IL-5 overexpressing mice have increased pulmonary eosinophilia and are more susceptible to *C. neoformans* infection as compared to WT mice. Furthermore, susceptibility of SP-D$^{-/-}$ mice to *C. neoformans* infection could be restored to that of WT mice by increasing IL-5 and eosinophils, via crossing the IL-5 overexpressing mice with SP-D$^{-/-}$ mice. Together, these studies support the conclusion that SP-D increases susceptibility to *C. neoformans* infection by promoting *C. neoformans*-driven pulmonary IL-5 and eosinophil infiltration.

Downloaded from http://iai.asm.org/ on November 28, 2020 by guest

IAI Accepts published online ahead of print

Downloaded from http://iai.asm.org/ on November 28, 2020 by guest

42 **Introduction**

43

44 *Cryptococcus neoformans* is an opportunistic fungal pathogen of the respiratory tract. It
45 is the leading cause of fungal meningoencephalitis, with one million infections and
46 600,000 attributable deaths occurring annually. *C. neoformans* is especially prevalent in
47 Sub-Saharan Africa where it causes approximately 30% of the deaths of HIV/AIDS
48 victims (1). Because *C. neoformans* is an opportunistic respiratory pathogen, an
49 immune-competent host is generally able to control the infection within the lung.
50 Conversely, when a host becomes immune-compromised the fungi disseminate out of the
51 lung, through the blood, and into the central nervous system (CNS), where uncontrolled
52 growth of cryptococcal organisms typically results in host morbidity and mortality.
53 The nature of the immune response is a critical determinant of host outcome
54 during *C. neoformans* pathogenesis. For example, Th1-skewed immune responses are
55 generally considered host-protective, while Th2-biased immune responses, characterized
56 by high IL-4, IL-5, and eosinophil expression, are non-protective in the context of *C.*
57 *neoformans* infection (2-8). Furthermore, an over-exuberant inflammatory response can
58 lead to complications such as cryptococcal immune reconstitution inflammatory
59 syndrome (IRIS) (9-11). Thus fine-tuned regulation of the inflammatory response is
60 necessary to ensure a favorable outcome for the host against *C. neoformans* infection.
61 Although it has a proclivity for the CNS, *C. neoformans* is a respiratory pathogen
62 that is normally encountered as an aerosol in the environment. Thus cells and proteins of
63 the lung provide the first line of defense against this potentially fatal pathogen. One class
64 of proteins that can regulate immune responses in the lung is surfactant proteins.

IAI Accepts published online ahead of print

Although classically known for mediating relief of surface tension in alveolar air spaces, two of the four defined surfactant proteins are now established in the literature as possessing immunomodulatory functions. Specifically, SP-A and SP-D, both members of the collectin family of proteins, are able to interact with pathogens and regulate immune responses. During bacterial and viral infections, as well as allergic reactions, SP-A and SP-D have been extensively shown to play protective roles that benefit the host (reviewed in Ref. (12)).

In contradiction to this host-protective paradigm, we have shown that SP-D$^{-/-}$ mice are less susceptible than wild-type (WT) mice to *C. neoformans*, and thus SP-D is considered detrimental to the host during *C. neoformans* infection (13, 14). Our studies have further demonstrated that SP-D$^{-/-}$ mice survive longer and have lower fungal burden than WT control animals. SP-D can opsonize *C. neoformans*, but increased phagocytosis has not been demonstrated to lead to increased fungal death. Instead, SP-D was shown to protect these fungi from macrophage-killing mechanisms, including reactive oxygen species (14). These observations led us to conclude that rather than playing a host-protective role, SP-D facilitates *C. neoformans* pathogenesis by protecting fungi from host immune responses, and that this fungal-protection was, in part, mediated via direct interaction with fungal cells. These findings prompted further *in vivo* investigations into the role of SP-D in mediating cryptococcal pathogenesis.

We hypothesized that SP-D exacerbates *C. neoformans* pathogenesis, at least in part, by dysregulating the early pulmonary immune response, causing heightened inflammation and detrimental cellular and cytokine responses. In the present study, using mice with genetically altered levels of IL-5, eosinophils, and SP-D, we examined the role

Downloaded from http://iai.asm.org/ on November 28, 2020 by guest

of IL-5 and eosinophil infiltration during *C. neoformans* infection. We concluded that SP-D increases susceptibility to pulmonary *C. neoformans* infection by acting as a natural immune enhancer of infection-driven IL-5 production and eosinophil infiltration in the lung, and that augmented levels of IL-5 and eosinophils contribute to increased host susceptibility to *C. neoformans*.

IAI Accepts published online ahead of print

Downloaded from http://iai.asm.org/ on November 28, 2020 by guest

IAI Accepts published online ahead of print

Materials and Methods

Mice. All mice were maintained in specific-pathogen free housing at Duke University. SP-D$^{-/-}$ (15) and IL-5TgxSP-D$^{-/-}$ and corresponding wild-type (WT) control mice (C57Bl/6J) were bred in-house. IL-5Tg (NJ.1638) (16) mice (kind gift of Dr. James Lee) were also bred in house and WT (C57Bl/6J) littermates were used as controls. As needed, additional C57Bl/6J mice were purchased from Jackson Laboratories (Bar Harbor, ME). For survival studies mice were infected between 6-8 weeks of age. For all other studies, mice were infected between 8-12 weeks of age. Both males and females were used. The animal protocol was approved by the Institutional Animal Care and Use Committee of Duke University (Protocol Number: A021-12-01). All surgery was performed under anesthesia with ketamine and xylazine, and every effort was made to minimize pain and suffering.

***C. neoformans* strains.** Mice were infected with H99 Stud, a highly virulent strain of *C. neoformans* serotype A that was created by passaging a mixed stock of *C. neoformans*, which included H99#1 (the original human isolate generated by Dr. John Perfect) through a rabbit (17). H99 Stud was used because of its effective and reproducible pathogenicity. H99 Stud was stored in a glycerol stock at -80°C. H99 Stud was maintained on yeast extract-peptone-dextrose (YPD) agar for up to one month. Liquid cultures were grown for 8 to 18 hours at 30°C with shaking (~250 rpm).

Downloaded from http://iai.asm.org/ on November 28, 2020 by guest

IAI Accepts published online ahead of print

***C. neoformans* infection.** For aerosol exposures, H99 Stud was grown at 30°C overnight in YPD liquid medium, then subcultured (1:100) for a second night, and inoculated onto V8 agar plates (made with 5% V8 original tomato juice, pH 5.0) in 10 µL spots (about 50 spots/plate) for 2-3 weeks. On the day of exposure, fungal colonies were gently removed with a cell scraper, dispersed into sterile PBS, centrifuged, and resuspended to $1x10^8$ cells/mL in sterile deionized water. *C. neoformans* was aerosolized using a 6-jet Collision nebulizer (CN25, BGI Incorporated). Mice were exposed to H99 Stud aerosol in a whole-body Madison chamber for 60 minutes at 95% relative humidity, in a BSL-3 biocontainment facility (NIAID Regional Biocontainment Laboratory at Duke). After exposure, mice were handled in class III and class II biosafety cabinets connected to the Madison chamber. They were then kept in hermetically sealed cages. Aerosol concentration of *C. neoformans* was measured via a BioSampler (SKC Incorporated) attached to the Madison chamber as previously described (18).

For intranasal instillation, H99 Stud was prepared as previously described (14). Briefly, *C. neoformans* cells were washed in sterile saline three times, counted, and resuspended to the desired cell density (between $5x10^4$ and $5x10^5$ yeast cells per mouse in 25-50 µL of saline as specified below). Mice were sedated with a ketamine (Ketaset®, Fort Dodge) (150 mg/kg) and xylazine (Anased®, Lloyd Incorporated) (10 mg/kg) mixture and hung gently by their incisors on a taut thread. The cell suspension was delivered by careful pipetting into one nostril. Sham-infected mice were given an equivalent volume of sterile saline. The mice were allowed to hang for five minutes after *C. neoformans* instillation.

Downloaded from http://iai.asm.org/ on November 28, 2020 by guest

IAI Accepts published online ahead of print

For fungal burden studies, histological analysis, survival studies, and flow cytometric analysis, mice were instilled with $5x10^4$ *C. neoformans* cells in 25-50 µL saline. For survival studies, mice were monitored for weight loss and general health per approved IACUC protocol. When mice lost more than 15% of initial body weight or became moribund they were humanely euthanized according to approved IACUC protocol. For BAL cellularity and cytokine analysis, mice were instilled with a higher dose of $5x10^5$ H99 Stud cells as a higher dose elicited greater differences in immune responses of WT and SP-$D^{-/-}$ mice.

BAL cellularity and cytokine analysis. On the day of organ harvest, mice were euthanized with Nembutol® (Oak Pharmaceuticals) or Euthasol® (Virbac Corporation) and exsanguinated via the renal artery. Lungs were perfused with a sufficient volume of sterile PBS to flush RBCs (5-10 mL) and then lavaged with 0.1 mM EDTA in PBS. A total of 6 mL lavage fluid was collected in 1 mL aliquots. BAL cells were centrifuged at 350 x *g*. Supernatant from the first 1 mL was stored at -80°C for cytokine analysis. BAL cells for each sample were pooled, counted, and adhered to slides via centrifuging 200 µL BAL in a Cytospin 2 (Shandon Incorporated) in at 400 rpm for 4 minutes. 50-100,000 cells were used for each cytospin. Cytospins were air dried, fixed with methanol, and stained with hematoxylin and eosin (H&E) for differential counting.

Cytokine concentrations were measured in cell-free supernatants acquired from the first 1 mL of collected BAL by multiplex assay using the 20-plex mouse inflammatory cytokine and chemokine panel (Invitrogen Life Sciences). For some experiments, IL-5 levels were assessed via ELISA (BD Biosciences: Pharmingen).

Downloaded from http://iai.asm.org/ on November 28, 2020 by guest

IAI Accepts published online ahead of print

Control samples showed comparable results for IL-5 concentration in both the bead-based multiplex and the ELISA assays.

Fungal burden analysis. On the day of harvest, mice were euthanized and exsanguinated as described above. For fungal burden analysis, lung tissue was excised and homogenized, and samples were diluted and plated onto YPD agar plates and incubated at room temperature or 30°C until colonies became large enough to count (usually 48-72 hours).

Tissue histology. Histological analyses were performed similarly to those previously described (19). Lungs were gravity inflated with 10% neutral buffered formalin (NBF), and paraffin embedded. 4-5um sections were deparaffinized and stained with hematoxylin and eosin. Blinded samples were scored by a veterinary pathologist for necrosis, hemorrhage, edema, *Cryptococcus*, and inflammation. Scores ranged from 0 to 8 with the score roughly representing the percentage of tissue involved (0 = 0%, 1 = 10%, 2 = 20%, etc.).

Lung tissue digests and immunophenotyping by flow cytometry. Lung digests for immunophenotyping were performed similarly to previously described methods (20). After perfusing and collecting BAL, the whole lung was excised and finely chopped with razor blades in a petri dish. Lung tissue was diluted in 4.5 mL HBSS with Ca^{2+} and Mg^{2+} and digested with DNase I and Collagenase XI (Roche). Single-cell suspensions were attained by passing the digested material through 40 um strainers and cells of

Downloaded from http://iai.asm.org/ on November 28, 2020 by guest

IAI Accepts published online ahead of print

hematopoietic-lineage were enriched by centrifuging the samples in a 4%/14.5% iodixanol gradient (Optiprep®; Axis-Shield). Cells were stained with the following antibodies: FITC Gr-1 (clone RB6-8C5; BD Biosciences), PE-Cy5.5 CD11c (clone N418; eBiosciences), APC-CD11b (clone M1/70; eBiosciences), Biotin MHC II (clone 2G9; BD Biosciences), and PE-Cy7 CD45 (clone 30-F11; BD Biosciences). PE-Texas Red Streptavidin (BD Biosciences) was used as the conjugate for biotin-labeled antibodies. Finally, cells were fixed with 10% NBF.

Immunophenotype list mode data were acquired on a BD-LSR II (BD Biosciences). Using Flow software (Treestar), sample data (FCS 3.0) were first analyzed for FSC-H versus FSC-A to gate on single cells. $CD45^+$ hematopoietic-lineage cells were then analyzed for Gr-1, CD11c, and MHC class II expression using bi-variate dot plots. PMNs were defined as $Gr\text{-}1^{hi}CD11c^{neg\text{-}lo}$ cells. We also assessed $CD11c^+MHCII^{int}$ cells (which should mainly consist of macrophages) and $CD11c^+MHCII^{hi}$ cells (which should mainly consist of dendritic cells). This gating strategy is based on the work of Lin*, et al*. (21). Cells that were $Gr\text{-}1^{neg\text{-}lo}$ $CD11c^{neg\text{-}lo}$MHC $II^{neg\text{-}lo}$ with high SSC were considered to be eosinophils (22, 23). The phenotype of these cells was confirmed by FACS and cytospin analysis with H&E staining. The remaining $CD45^+$ cells were designated "lymphocytes/other". Isotype-matched antibodies were used for control staining.

RNA isolation, reverse transcription (RT), and real-time PCR analysis. RNA was isolated from lung tissue with TRIzol reagent (Invitrogen) per manufacturer's protocol, followed by chloroform extraction and isopropanol precipitation. Equal amounts of RNA were reverse-transcribed with MMLV and random primers. Real-time PCR was

Downloaded from http://iai.asm.org/ on November 28, 2020 by guest

performed with the double-stranded DNA probe SYBR green in a two-step reaction on a Bio-Rad CFX96 machine. Results were normalized to β-actin RNA as an internal control and analyzed by the $2^{-\Delta\Delta CT}$ method. The oligonucleotide primers for β-actin were 5'-GATTACTGCTCTGGCTCCTAG-3' (Forward) and 5'-GACTCATCGTACTCCTGCTTGC-3' (Reverse). The oligonucleotide primers for IL-5 were 5'-AGCACAGTGGTGAAAGAGACCTT-3' (Forward) and 5'-TCCAATGCATAGCTGGTGATTT-3' (Reverse).

Statistical analysis. Statistical analyses were performed with GraphPad Prism software (version 5.0) or SAS Statview software. To compare two groups, data were analyzed by two-tailed Student's T test. For multiple comparisons, data were analyzed by one-way or two-way ANOVA followed by Bonferroni's or Tukey's posttest correction. Survival studies were assessed via Kaplan-Meier survival curve analysis with the Mantel-Cox test. A *P*-value of < 0.05 was considered significant.

IAI Accepts published online ahead of print

Downloaded from http://iai.asm.org/ on November 28, 2020 by guest

IAI Accepts published online ahead of print

Downloaded from http://iai.asm.org/ on November 28, 2020 by guest

Results

SP-D$^{-/-}$ mice are less susceptible than WT mice to *C. neoformans* in an aerosol exposure model. SP-D is a constitutively expressed pulmonary protein that is immediately available to interact with *C. neoformans* after the pathogen enters the lung. Our previous studies used intranasal instillation of inoculum by directly pipetting a suspension of cryptococcal cells into the nostrils of lightly sedated mice. Naturally occurring *C. neoformans* infections, however, generally arise after inhalation of aerosolized *C. neoformans* in the environment. Thus, we asked whether a more natural route of exposure to *C. neoformans* would yield comparable results to intranasal instillation; that is, whether SP-D would facilitate *C. neoformans* pathogenesis after exposure to aerosolized fungal cells.

WT and SP-D$^{-/-}$ mice were simultaneously exposed to aerosolized *C. neoformans* in a Madison whole-body exposure chamber (see materials and methods). The average aerosol concentration of three independent exposures was 8±2 CFU/mL. The fungal load was quantified at 1 hour, 24 hours, 10 days, 14 days, and 21 days post-infection. At early stages of infection (1 hour and 24 hours), WT and SP-D$^{-/-}$ mice had similar fungal loads, but as the infection progressed fungal loads were higher in WT mice compared to SP-D$^{-/-}$ mice with a significant difference between strains apparent at 14 and 21 days post-infection (Figure 1A). Histological analysis at day 21-post-infection confirmed increased pathology in WT mice compared to SP-D$^{-/-}$ mice (Figure 1B-C and Table 1). These data corroborate that SP-D facilitates *C. neoformans* pathogenesis across different models of

IAI Accepts published online ahead of print

Downloaded from http://iai.asm.org/ on November 28, 2020 by guest

infection and support the continued use of the more accessible intranasal instillation method as a model infection route for *C. neoformans* in mice.

SP-D$^{-/-}$ mice have a decreased pulmonary cellular immune response to *C. neoformans* compared to WT mice. To further characterize the effect of SP-D during *C. neoformans* infection, the pulmonary cellular response in WT and SP-D$^{-/-}$ mice was assessed. Using immunophenotyping and polychromatic flow cytometry, myeloid cell infiltration in both BAL and interstitial lung tissue was quantified at three and seven days post-*C. neoformans* infection. In lung interstitium and BAL, the absolute number of infiltrating CD45^{+} cells (hematopoietic lineage cells) in both WT and SP-D$^{-/-}$ mice increased with infection (Figure 2A-B). This CD45^{+} cell lung infiltration was statistically lower in infected SP-D$^{-/-}$ mice than in infected WT control mice. A similar trend was observed in BAL. Detailed analysis of the frequency of myeloid cell populations within the lung CD45^{+} compartment revealed that the difference between infected WT and SP-D$^{-/-}$ mice could not be accounted for by differences in the proportion of polymorphonuclear cells (PMNs) (Figure 2C-D), CD11c^{+}MHCII^{int} cells (likely macrophages) (Figure 2E-F), nor CD11c^{+}MHCII^{hi} cells (likely dendritic cells) (Figure 2G-H). However, a large population of MHC II$^{neg\text{-}low}$/CD11c$^{neg\text{-}low}$/SSC^{hi} cells was observed that was lower in infected SP-D$^{-/-}$ mice than in infected WT mice (data not shown). Since this population of cells was undetermined by our flow cytometry panels, additional cytospin analysis with H&E staining was conducted and revealed that these cells were eosinophils (Figure 3E-H). Thus, eosinophils account for the majority of the CD45^{+} pulmonary cell influx post-*C. neoformans* infection and SP-D$^{-/-}$ mice had reduced frequencies of eosinophil infiltration compared to WT mice. SP-D$^{-/-}$ mice also had lower

IAI Accepts published online ahead of print

absolute numbers of eosinophils after seven days of *C. neoformans* infection compared to WT mice in the interstitium ($24x10^5 \pm 5x10^5$ cells in WT mice and $5x10^5 \pm 1x10^5$ cells in SP-D$^{-/-}$ mice) and BAL ($9x10^5 \pm 3x10^5$ cells in WT mice and $7x10^5 \pm 3x10^5$ cells in SP-D$^{-/-}$ mice), which further endorsed the substantial differences between WT and SP-D$^{-/-}$ mice. WT and SP-D$^{-/-}$ mice did not have significantly different frequencies of the remainder of CD45$^+$ cells, which were primarily lymphocytes.

To confirm the findings of the flow cytometric analysis, eosinophils were quantified by classical cytospin/histologic analysis of BAL cells. Eosinophils were significantly lower in infected SP-D$^{-/-}$ mice compared to infected WT mice at day seven (Figure 3A). The resultant eosinophilia values were lower by cytospin analysis than they were by FACS analysis: this is because the design of the flow cytometry panel tends to underestimate the number of eosinophils. Notably, the fold differences were similar using both methods (*i.e.* WT mice had more eosinophils than SP-D$^{-/-}$ mice, post infection). Thus, we concluded that eosinophils dominate the lung environment after *C. neoformans* infection and that SP-D enhances eosinophilia during *C. neoformans* infection in both the interstitial and alveolar compartments of the lung.

SP-D$^{-/-}$ mice have altered pulmonary cytokine/chemokine responses to *C. neoformans* compared to WT mice. To determine the effect of SP-D on the lung inflammatory cytokine response to *C. neoformans*, we quantified levels of twenty cytokines in BAL fluid from WT and SP-D$^{-/-}$ mice seven days post-infection (Table 2). In WT mice, *C. neoformans* infection stimulated higher production of IFN-γ, TNF-α, IL-4, IL-5, IL-6, IL-12, IL-13, IP-10, and MCP-1 compared to sham-infected WT mice. Of

Downloaded from http://iai.asm.org/ on November 28, 2020 by guest

IAI Accepts published online ahead of print

these infection-induced cytokines/chemokines, IFN-γ, IL-4, IL-6, and IL-13 were produced at comparable levels in SP-D$^{-/-}$ mice, suggesting that SP-D does not alter the production of these immune mediators seven days post-*C. neoformans* infection.

Of interest, IL-5, IP-10, and MCP-1 were significantly higher in SP-D$^{-/-}$ mice compared to WT mice after seven days of infection, revealing a possible mechanism by which SP-D protein may cause suppression of some cytokines/chemokines during *C. neoformans* infection. Additionally, *C. neoformans* infection stimulated production of MIG and MIP-1α specifically in SP-D$^{-/-}$ mice. Since neither was detected in WT mice, this finding suggests that SP-D suppresses certain host cytokine/chemokine responses in fungal infection. Conversely, *C. neoformans* infection stimulated TNF-α production in WT mice significantly more than in SP-D$^{-/-}$ mice, showing that SP-D might enhance TNF-α expression. IL-17, KC, GM-CSF, IL-1α, IL-1β, IL-2, and IL-10 were not induced by *C. neoformans* infection (data not shown for GM-CSF, IL-1α, IL-1β, IL-2, and IL-10). Overall, cytokine/chemokine analysis did not reveal a clear bias toward Th1 or Th2 responses; rather SP-D has a dysregulating, sometimes stimulating and sometimes suppressing, effect on certain chemokines and Th1 cytokines seven days post-infection.

Interestingly, higher IL-5 levels in SP-D$^{-/-}$ mice compared to WT mice seven days post-infection was incongruent with our cellular analyses showing higher eosinophilia in WT mice. We postulated that there were earlier increases in IL-5 that could account for the elevated eosinophilia observed at seven days post-infection. Thus IL-5 levels were quantified three days post-infection in both strains of mice. As predicted, BAL IL-5 was highly induced in WT mice three days post-infection compared to SP-D$^{-/-}$ mice (Figure 3B). This early rise in lung IL-5 protein levels in WT mice corresponded with increased

Downloaded from http://iai.asm.org/ on November 28, 2020 by guest

IAI Accepts published online ahead of print

IL-5 steady-state mRNA levels in lung tissue of WT mice during day two post-infection (Figure 3C). This early induction of IL-5 expression levels was not detected in SP-D$^{-/-}$ mice. Additionally, it should be noted that multiplex analysis was performed at day three for the same cytokine panel as day seven, and we did not observe any significant differences that seemed as relevant to eosinophilia as the results with IL-5 (data not shown).

To determine whether IL-5 was necessary for the observed eosinophil recruitment in this model, IL-5 neutralizing antibodies were administered by i.p. injection on the day of infection and eosinophilia was measured seven days post-infection (Figure 3D). Eosinophilia induced by *C. neoformans* infection was drastically reduced in both WT and SP-D$^{-/-}$ mice with antibody administration, thus affirming the critical importance of IL-5 for eosinophil recruitment during acute *C. neoformans* infection. Together these data demonstrate that delayed IL-5 induction accounts for decreased eosinophilia in SP-D$^{-/-}$ mice as compared to WT mice.

Mice overexpressing IL-5 and eosinophils are more susceptible to *C. neoformans* than WT mice. Having established that IL-5 and eosinophil levels are augmented more in WT mice than SP-D$^{-/-}$ mice during the early phase of infection, it was next necessary to define the role of IL-5 and eosinophils during cryptococcal pathogenesis in relationship to SP-D. Thus IL-5 Transgenic (Tg) mice that overproduce IL-5 under a T cell specific promoter and therefore have a constitutive overabundance of eosinophils in the peripheral blood were infected with $5x10^4$ H99 Stud cells for histological studies, pulmonary fungal burden comparisons, and survival analyses (16). As predicted, after *C. neoformans*

Downloaded from http://iai.asm.org/ on November 28, 2020 by guest

IAI Accepts published online ahead of print

infection, IL-5Tg mice displayed high overexpression of both IL-5 and eosinophils in BAL fluid (Figure S1). At seven days post-infection, fungal burden was significantly higher in IL-5Tg mice (Figure 4A). Histological analysis confirmed the fungal burden analysis and revealed that IL-5Tg mice had increased necrosis and inflammation compared to WT mice (Table 3 and Figure 6). Finally, IL-5Tg mice died more rapidly in survival studies compared to WT control mice (Figure 4B). These data indicated that augmentation of IL-5 production and resulting eosinophilia contributed significantly to *C. neoformans* pathogenesis.

IL-5 overexpression reverses the SP-D$^{-/-}$ response to *C. neoformans.* We next examined the *in vivo* linkage between IL-5 and SP-D by asking whether augmenting IL-5 levels in SP-D deficient mice could reverse the SP-D$^{-/-}$ phenotype and result in increased susceptibility to *C. neoformans* infection. We created IL-5TgxSP-D$^{-/-}$ mice and assessed fungal burden, histology, and survival in these mice. Cytokine and cytospin analysis confirmed high levels of eosinophils and IL-5 seven days post-infection in IL-5TgxSP-D$^{-/-}$ mice (Figure S1). At fourteen days post-infection, IL-5TgxSP-D$^{-/-}$ mice had higher than SP-D$^{-/-}$ mice, and lower than IL-5Tg mice similar fungal burden to WT mice (Figure 5A). Survival analysis, likewise, revealed that IL-5TgxSP-D$^{-/-}$ mice were significantly more susceptible to *C. neoformans* than SP-D$^{-/-}$ mice, less susceptible than IL-5Tg mice, and not statistically different from WT mice (Figure 5B). Histological analysis confirmed that IL-5TgxSP-D$^{-/-}$ mice were less susceptible to *C. neoformans* than IL-5Tg mice as they had lower levels of hemorrhage, necrosis, edema, cryptococcal cells, and inflammation (Table 3 and Figure 6). Together, these data demonstrated that

Downloaded from http://iai.asm.org/ on November 28, 2020 by guest

overexpression of IL-5, and thus eosinophils, restores SP-D$^{-/-}$ mice to the WT phenotype and supports the conclusion that SP-D protein augments *C. neoformans* disease in the murine host by promoting an excessive IL-5 expression and eosinophil infiltration in response to this fungal infection.

IAI Accepts published online ahead of print

Downloaded from http://iai.asm.org/ on November 28, 2020 by guest

IAI Accepts published online ahead of print

Downloaded from http://iai.asm.org/ on November 28, 2020 by guest

362 **Discussion**

363

364 SP-D is well documented as a host-protective immunoregulatory protein, yet our
365 previous studies have demonstrated that SP-D fails to protect mice against *C. neoformans*
366 by promoting fungal growth and survival to the detriment of the host (13, 14). The
367 uniqueness of the interaction between SP-D and *C. neoformans* prompted further
368 investigation into the mechanisms by which SP-D affects host outcome in the face of *C.*
369 *neoformans* infection. Because of the immunoregulatory role of SP-D, we hypothesized
370 that one mechanism by which SP-D increases susceptibility to *C. neoformans* may be
371 through dysregulation of host immune responses. Analysis of *C. neoformans* infection in
372 WT and SP-D$^{-/-}$ mice revealed that SP-D increases inflammatory cell infiltrate and
373 dysregulates the balance of pulmonary cytokines in response to *C. neoformans*. We
374 specifically identified a role for SP-D in augmenting eosinophils and IL-5, an eosinophil
375 recruitment and survival cytokine, during active *C. neoformans* infection. Select mutant
376 mouse models were used to further examine the roles of IL-5, eosinophils, and SP-D
377 during *C. neoformans* pathogenesis. Together these studies demonstrate a dynamic
378 interplay between SP-D, IL-5, and eosinophils in determining the outcome of *C.*
379 *neoformans* disease during the critical early phase of pulmonary infection.

380 To mimic the natural route of infection, we examined the ability of SP-D to
381 facilitate cryptococcal pathogenesis after exposure to aerosolized *C. neoformans* cells.
382 WT mice were more susceptible to aerosol exposures of *C. neoformans* than SP-D$^{-/-}$ mice
383 (Figure 1). This confirmed that the ability of SP-D to affect *C. neoformans* disease is free
384 of artifact due to the intranasal instillation method, corroborating our previous survival

IAI Accepts published online ahead of print

and fungal burden analyses with intranasal infections and firmly establishing that SP-D increases susceptibility to *C. neoformans* infection (13). This conclusion is further supported by models using inducible SP-D mice and via rescue studies in which SP-D protein instilled in the nostrils of SP-D$^{-/-}$ mice increased susceptibility of SP-D$^{-/-}$ mice to the levels of WT mice (13). These findings clearly validate the intranasal instillation method as a biologically relevant and robust model for early pulmonary *C. neoformans* disease and, thus, in the immunological studies that followed, we used the traditional and more readily accessible intranasal method.

Immunophenotyping revealed *C. neoformans* induced higher levels of inflammatory (CD45^{+}) cells in WT mice compared to SP-D$^{-/-}$ mice (Figure 2), indicating that SP-D contributes to *C. neoformans* pathogenesis by exacerbating over-exuberant immune responses that might be detrimental to the host. This was in agreement with our hypothesis. Furthermore, the presence of SP-D in WT mice was associated with increased eosinophil recruitment (Figure 3). This is in direct contrast with the mold, *Aspergillus fumigatus*, a medically relevant fungal species that has been studied extensively in the context of SP-D, in which the main role of SP-D is to suppress excessive inflammation, including eosinophilia, thereby reducing damage to the host (24-28). Thus, we postulate that while SP-D protects against *A. fumigatus* by dampening and thus preventing over-exuberant immune responses and excessive eosinophilia after *A. fumigatus* exposure, it conversely contributes to *C. neoformans* pathogenesis by augmenting eosinophilic responses to *C. neoformans* leading to excessive inflammation and potentially damaging the surrounding host tissue. The histology from this study and

Downloaded from http://iai.asm.org/ on November 28, 2020 by guest

IAI Accepts published online ahead of print

from previous studies support this hypothesis (13), as WT mice displayed more extensive damage within the pulmonary airspaces than SP-D$^{-/-}$ mice (Figure 1 and Table 1).

In addition to analysis of the cellular immune response, we also examined cytokine/chemokine responses after *C. neoformans* infection. Multiple pro-inflammatory markers were induced by *C. neoformans* infection in both WT and SP-D$^{-/-}$ mice, with several key chemokines and Th1 cytokines expressed to a lesser extent in WT mice (Table 2). These observations indicate that SP-D may contribute to the susceptibility of WT mice by suppressing key inflammatory cytokines and chemokines, such as IL-12, IP-10, MIP-1α, MIG, and MCP-1, which are normally protective against *C. neoformans* (4-6, 29-34).

Following the immune phenotyping observations of eosinophil differences in the lung interstitial and lavage compartments, specific examination of IL-5 levels showed delayed IL-5 induction in SP-D$^{-/-}$ compared to WT mice (Figure 3 and Table 2). These data revealed a dynamic role for SP-D in modulating IL-5 expression and we postulated that a delayed IL-5 response in SP-D$^{-/-}$ mice resulted in decreased eosinophilia as detected seven days after infection. Furthermore, IL-5 blockade studies presented herein confirm that IL-5 is required for eosinophilia at an early stage of acute infection. This is in accordance with previous work in which IL-5 was also necessary for eosinophilia in a chronic *C. neoformans* infection model (8). During chronic *C. neoformans* infection, CD4^{+} T cells were critical producers of IL-5, but we expect that other cell types are a more significant source of IL-5 during the initial stages of an acute response. Potential candidates include lung stromal cells, such as epithelial cells (35, 36), and innate immune

Downloaded from http://iai.asm.org/ on November 28, 2020 by guest

IAI Accepts published online ahead of print

cells, such as mast cells, monocytes, or a newly identified IL-5 producing non-T lymphoid cell type that can rapidly produce this cytokine (37-40).

The role of IL-5 and eosinophils during *C. neoformans* pathogenesis has remained elusive. Along with the widely published fact that eosinophilia has often been associated with ineffective immune responses against *C. neoformans*, it has been shown that eosinophils bind *C. neoformans* in the presence of opsonizing antibodies (41), late phase *C. neoformans*-induced pulmonary eosinophilia is IL-5 dependent (8), and eosinophils have *C. neoformans*-derived antigen presenting capabilities (42, 43). Recently eosinophils were found to be important producers of IL-4, and thus are contributors to non-protective Th2 responses (44). It has remained unclear whether IL-5 and eosinophils are mere bystanders during an otherwise pathogenic Th2 process or whether they were active contributors to *C. neoformans* disease. The present studies help to elucidate the role of eosinophils and IL-5 in *C. neoformans* pathogenesis in the context of SP-D. Overexpression of IL-5 and a large resultant eosinophil population significantly increased host susceptibility to *C. neoformans* (Figure 4). This is in contrast with recent bacterial studies that demonstrated that IL-5Tg mice were protected against bacterial infection due to bactericidal capabilities of eosinophils (45). Furthermore, studies with IL-5TgxSP-D$^{-/-}$ mice determined that augmenting expression of IL-5 and eosinophils in SP-D$^{-/-}$ mice was sufficient to restore susceptibility to *C. neoformans*, providing strong evidence that decreased IL-5 and eosinophils are an important part of explaining the mechanistic role of SP-D in promoting *C. neoformans* pathogenesis (Figure 5). However, we did examine whether components of these interactions had an impact on the phenotype. When fungal burden and survival were additionally assessed in PHIL (eosinophil-deficient) and IL5-/-

Downloaded from http://iai.asm.org/ on November 28, 2020 by guest

IAI Accepts published online ahead of print

mice after *C. neoformans* infection (data not shown) we found no or minimal impact, respectively, on outcome. Taken together, these data suggest that IL-5, eosinophils, and SP-D work together to determine host fate in *C. neoformans* disease and highlight the importance of balance in host cytokine production, collectin presence, and host cell influx to the site of infection during specific microbial assaults.

In the present study, SP-D acts as a natural enhancer of *C. neoformans*-driven IL-5 production and eosinophil infiltration in the lung, leading to increased host susceptibility. This model is in contrast to *A. fumigatus* (24-27, 46) in which SP-D plays a host-protective role by reducing Th2 responses. The ability of SP-D to act as a suppressor of IL-5 and eosinophilia in *A. fumigatus* models, while acting as an enhancer of IL-5 and eosinophilia during *C. neoformans* infection can be explained by the dual role of SP-D in inflammation. SP-D can act as an anti-inflammatory molecule when present as a dodecamer that interacts with SIRPα. Conversely, SP-D can act as a pro-inflammatory molecule leading to NF-κB activation and proinflammatory signaling cascades after *S*-nitrosylation, trimer formation and interaction with CD91/calreticulin (47). Previous work showing that oligomeric SP-D inhibits eosinophil chemotaxis, while *S*-nitrosylated SP-D does not, supports this dual role paradigm for SP-D in eosinophilia (48, 49). Future studies should focus on gaining a deeper understanding of the dual role of SP-D in infection and inflammation by examining the oligomeric structure and post-translational modifications of SP-D during both *C. neoformans* and *A. fumigatus* infections. Although both are pathogenic fungi, they diverge widely in nucleic acid sequence, morphology, pathogenic features, and host susceptibility. Comparing the status of SP-D protein in both models should lend significant insight into fundamental

Downloaded from http://iai.asm.org/ on November 28, 2020 by guest

differences about how SP-D differentially affects host outcome in the face of two divergent types of fungal infections.

In conclusion, the effects of SP-D, IL-5, and eosinophils are interwoven to establish the early innate immune response to this encapsulated yeast and promote fungal pathogenesis. Future studies focused on disrupting the interactions of this triad of factors could suggest potential therapeutic strategies leading to disease prevention.

IAI Accepts published online ahead of print

Downloaded from http://iai.asm.org/ on November 28, 2020 by guest

IAI Accepts published online ahead of print

482 **Acknowledgements**

483 This work was supported by Public Health Service grants R01-HL30923 to J.R.W. and
484 R01-AI73896 to J.R.P from the National Institutes of Health.

485 The authors would like to thank Julia L. Nugent, Kristina Riebe, and Melissa
486 Ventevogel for technical assistance, particularly with breeding, genotyping, and handling
487 mice. We also thank Ching-Ju Chen, Sarah Seay, and Rosemarie Asrican for technical
488 assistance with aerobiology studies, and Patrice McDermott for technical assistance with
489 flow cytometry studies.

490 Aerosol challenges, flow cytometry, and cytokine profiling were performed in the
491 NIAID Regional Biocontainment Laboratory at Duke (UC6-AI058607, U54-AI057157,
492 P30-AI051445) by the Duke Human Vaccine Institute (DHVI) Aerobiology Shared
493 Resource Facility, the DHVI Flow Cytometry Shared Resource Facility under the
494 direction of John F. Whitesides, and the DHVI Immune Reconstitution & Biomarker
495 Analysis Shared Resource Facility, respectively.

496

497

Downloaded from http://iai.asm.org/ on November 28, 2020 by guest

IAI Accepts published online ahead of print

References

1. **Park BJ, Wannemuehler KA, Marston BJ, Govender N, Pappas PG, Chiller TM.** 2009. Estimation of the current global burden of cryptococcal meningitis among persons living with HIV/AIDS. AIDS **23:**525-530.

2. **Jain AV, Zhang Y, Fields WB, McNamara DA, Choe MY, Chen Gh, Erb-Downward J, Osterholzer JJ, Toews GB, Huffnagle GB, Olszewski MA.** 2009. Th2 but Not Th1 Immune Bias Results in Altered Lung Functions in a Murine Model of Pulmonary *Cryptococcus neoformans* Infection. Infection and Immunity **77:**5389-5399.

3. **Muller U, Stenzel W, Kohler G, Werner C, Polte T, Hansen G, Schutze N, Straubinger RK, Blessing M, McKenzie AN, Brombacher F, Alber G.** 2007. IL-13 induces disease-promoting type 2 cytokines, alternatively activated macrophages and allergic inflammation during pulmonary infection of mice with *Cryptococcus neoformans*. J Immunol **179:**5367-5377.

4. **Hardison SE, Ravi S, Wozniak KL, Young ML, Olszewski MA, Wormley FL, Jr.** 2010. Pulmonary infection with an interferon-gamma-producing *Cryptococcus neoformans* strain results in classical macrophage activation and protection. Am J Pathol **176:**774-785.

5. **Chen Gh, McNamara DA, Hernandez Y, Huffnagle GB, Toews GB, Olszewski MA.** 2008. Inheritance of Immune Polarization Patterns Is Linked to Resistance versus Susceptibility to *Cryptococcus neoformans* in a Mouse Model. Infection and Immunity **76:**2379-2391.

Downloaded from http://iai.asm.org/ on November 28, 2020 by guest

IAI Accepts published online ahead of print

6. **Zhang Y, Wang F, Tompkins KC, McNamara A, Jain AV, Moore BB, Toews GB, Huffnagle GB, Olszewski MA.** 2009. Robust Th1 and Th17 Immunity Supports Pulmonary Clearance but Cannot Prevent Systemic Dissemination of Highly Virulent *Cryptococcus neoformans* H99. American Journal Of Pathology **175:**2489-2500.

7. **Wozniak KL, Ravi S, Macias S, Young ML, Olszewski MA, Steele C, Wormley FL.** 2009. Insights into the mechanisms of protective immunity against *Cryptococcus neoformans* infection using a mouse model of pulmonary cryptococcosis. PLoS One **4:**e6854.

8. **Huffnagle GB, Boyd MB, Street NE, Lipscomb MF.** 1998. IL-5 is required for eosinophil recruitment, crystal deposition, and mononuclear cell recruitment during a pulmonary *Cryptococcus neoformans* infection in genetically susceptible mice (C57BL/6). J Immunol **160:**2393-2400.

9. **Wiesner DL, Boulware DR.** 2011. Cryptococcus-Related Immune Reconstitution Inflammatory Syndrome(IRIS): Pathogenesis and Its Clinical Implications. Current fungal infection reports **5:**252-261.

10. **da Cunha Colombo ER, Mora DJ, Silva-Vergara ML.** 2011. Immune reconstitution inflammatory syndrome (IRIS) associated with *Cryptococcus neoformans* infection in AIDS patients. Mycoses **54:**e178-182.

11. **Skiest DJ, Hester LJ, Hardy RD.** 2005. Cryptococcal immune reconstitution inflammatory syndrome: report of four cases in three patients and review of the literature. The Journal of infection **51:**e289-297.

Downloaded from http://iai.asm.org/ on November 28, 2020 by guest

IAI Accepts published online ahead of print

542 12. **Crouch EC.** 1998. Collectins and pulmonary host defense. Am J Respir Cell Mol
543 Biol **19:**177-201.
544 13. **Geunes-Boyer S, Beers MF, Perfect JR, Heitman J, Wright JR.** 2012.
545 Surfactant Protein D Facilitates *Cryptococcus neoformans* Infection. Infect
546 Immun **80:**2444-2453.
547 14. **Geunes-Boyer S, Oliver TN, Janbon G, Lodge JK, Heitman J, Perfect JR,**
548 **Wright JR.** 2009. Surfactant Protein D Increases Phagocytosis of Hypocapsular
549 *Cryptococcus neoformans* by Murine Macrophages and Enhances Fungal
550 Survival. Infection and Immunity **77:**2783-2794.
551 15. **Korfhagen TR, Sheftelyevich V, Burhans MS, Bruno MD, Ross GF, Wert**
552 **SE, Stahlman MT, Jobe AH, Ikegami M, Whitsett JA, Fisher JH.** 1998.
553 Surfactant protein-D regulates surfactant phospholipid homeostasis in vivo. J Biol
554 Chem **273:**28438-28443.
555 16. **Lee NA, McGarry MP, Larson KA, Horton MA, Kristensen AB, Lee JJ.**
556 1997. Expression of IL-5 in thymocytes/T cells leads to the development of a
557 massive eosinophilia, extramedullary eosinophilopoiesis, and unique
558 histopathologies. J Immunol **158:**1332-1344.
559 17. **Morrow CA, Lee IR, Chow EW, Ormerod KL, Goldinger A, Byrnes EJ, 3rd,**
560 **Nielsen K, Heitman J, Schirra HJ, Fraser JA.** 2012. A unique chromosomal
561 rearrangement in the *Cryptococcus neoformans* var. grubii type strain enhances
562 key phenotypes associated with virulence. MBio **3**.
563 18. **Saini D, Hopkins GW, Chen CJ, Seay SA, Click EM, Lee S, Hartings JM,**
564 **Frothingham R.** 2011. Sampling port for real-time analysis of bioaerosol in

Downloaded from http://iai.asm.org/ on November 28, 2020 by guest

IAI Accepts published online ahead of print

whole body exposure system for animal aerosol model development. Journal of pharmacological and toxicological methods **63:**143-149.

19. **Steinbach WJ, Benjamin DK, Jr., Trasi SA, Miller JL, Schell WA, Zaas AK, Foster WM, Perfect JR.** 2004. Value of an inhalational model of invasive aspergillosis. Med Mycol **42:**417-425.

20. **Awasthi S.** 2010. Surfactant protein (SP)-A and SP-D as antimicrobial and immunotherapeutic agents. Recent Pat Antiinfect Drug Discov **5:**115-123.

21. **Lin KL, Suzuki Y, Nakano H, Ramsburg E, Gunn MD.** 2008. CCR2+ monocyte-derived dendritic cells and exudate macrophages produce influenza-induced pulmonary immune pathology and mortality. J Immunol **180:**2562-2572.

22. **Rose S, Misharin A, Perlman H.** 2012. A novel Ly6C/Ly6G-based strategy to analyze the mouse splenic myeloid compartment. Cytometry. Part A : the journal of the International Society for Analytical Cytology **81:**343-350.

23. **Milam JE, Herring-Palmer AC, Pandrangi R, McDonald RA, Huffnagle GB, Toews GB.** 2007. Modulation of the pulmonary type 2 T-cell response to *Cryptococcus neoformans* by intratracheal delivery of a tumor necrosis factor alpha-expressing adenoviral vector. Infect Immun **75:**4951-4958.

24. **Kishore U, Madan T, Sarma PU, Singh M, Urban BC, Reid KBM.** 2002. Protective roles of pulmonary surfactant proteins, SP-A and SP-D, against lung allergy and infection caused by *Aspergillus fumigatus*. Immunobiology **205:**610-618.

Downloaded from http://iai.asm.org/ on November 28, 2020 by guest

IAI Accepts published online ahead of print

25. **Madan T, Kishore U, Singh M, Strong P, Hussain EM, Reid KBM, Sarma PU.** 2001. Protective Role of Lung Surfactant Protein D in a Murine Model of Invasive Pulmonary Aspergillosis. Infection and Immunity **69:**2728-2731.

26. **Madan T, Reid KB, Clark H, Singh M, Nayak A, Sarma PU, Hawgood S, Kishore U.** 2010. Susceptibility of mice genetically deficient in SP-A or SP-D gene to invasive pulmonary aspergillosis. Mol Immunol **47:**1923-1930.

27. **Madan T, Reid KB, Singh M, Sarma PU, Kishore U.** 2005. Susceptibility of mice genetically deficient in the surfactant protein (SP)-A or SP-D gene to pulmonary hypersensitivity induced by antigens and allergens of *Aspergillus fumigatus*. J Immunol **174:**6943-6954.

28. **Brandt E, Mingler M, Stevenson M, Wang N, Khuranahershey G, Whitsett J, Rothenberg M.** 2008. Surfactant protein D alters allergic lung responses in mice and human subjects. Journal of Allergy and Clinical Immunology **121:**1140-1147.e1142.

29. **Olszewski MA, Huffnagle GB, Traynor TR, McDonald RA, Cook DN, Toews GB.** 2001. Regulatory effects of macrophage inflammatory protein 1alpha/CCL3 on the development of immunity to *Cryptococcus neoformans* depend on expression of early inflammatory cytokines. Infect Immun **69:**6256-6263.

30. **Olszewski MA, Huffnagle GB, McDonald RA, Lindell DM, Moore BB, Cook DN, Toews GB.** 2000. The role of macrophage inflammatory protein-1 alpha/CCL3 in regulation of T cell-mediated immunity to *Cryptococcus neoformans* infection. J Immunol **165:**6429-6436.

Downloaded from http://iai.asm.org/ on November 28, 2020 by guest

31. **Hardison SE, Herrera G, Young ML, Hole CR, Wozniak KL, Wormley FL, Jr.** 2012. Protective immunity against pulmonary cryptococcosis is associated with STAT1-mediated classical macrophage activation. J Immunol **189:**4060-4068.

32. **Huffnagle GB, Strieter RM, Standiford TJ, McDonald RA, Burdick MD, Kunkel SL, Toews GB.** 1995. The role of monocyte chemotactic protein-1 (MCP-1) in the recruitment of monocytes and CD4+ T cells during a pulmonary *Cryptococcus neoformans* infection. J Immunol **155:**4790-4797.

33. **Vecchiarelli A, Pietrella D, Bistoni F, Kozel TR, Casadevall A.** 2002. Antibody to *Cryptococcus neoformans* capsular glucuronoxylomannan promotes expression of interleukin-12Rbeta2 subunit on human T cells in vitro through effects mediated by antigen-presenting cells. Immunology **106:**267-272.

34. **Wormley FL, Perfect JR, Steele C, Cox GM.** 2007. Protection against Cryptococcosis by Using a Murine Gamma Interferon-Producing *Cryptococcus neoformans* Strain. Infection and Immunity **75:**1453-1462.

35. **Salvi S, Semper A, Blomberg A, Holloway J, Jaffar Z, Papi A, Teran L, Polosa R, Kelly F, Sandstrom T, Holgate S, Frew A.** 1999. Interleukin-5 production by human airway epithelial cells. Am J Respir Cell Mol Biol **20:**984-991.

36. **Wu CA, Peluso JJ, Zhu L, Lingenheld EG, Walker ST, Puddington L.** 2010. Bronchial epithelial cells produce IL-5: implications for local immune responses in the airways. Cell Immunol **264:**32-41.

IAI Accepts published online ahead of print

Downloaded from http://iai.asm.org/ on November 28, 2020 by guest

IAI Accepts published online ahead of print

630 37. **Ikutani M, Yanagibashi T, Ogasawara M, Tsuneyama K, Yamamoto S,**
631 **Hattori Y, Kouro T, Itakura A, Nagai Y, Takaki S, Takatsu K.** 2012.
632 Identification of innate IL-5-producing cells and their role in lung eosinophil
633 regulation and antitumor immunity. J Immunol **188:**703-713.
634 38. **Plaut M, Pierce JH, Watson CJ, Hanley-Hyde J, Nordan RP, Paul WE.** 1989.
635 Mast cell lines produce lymphokines in response to cross-linkage of Fc epsilon RI
636 or to calcium ionophores. Nature **339:**64-67.
637 39. **Okayama Y, Kobayashi H, Ashman LK, Holgate ST, Church MK, Mori M.**
638 1997. Activation of eosinophils with cytokines produced by lung mast cells. Int
639 Arch Allergy Immunol **114 Suppl 1:**75-77.
640 40. **Diedrich CR, Mattila JT, Flynn JL.** 2013. Monocyte-Derived IL-5 Reduces
641 TNF Production by Mycobacterium tuberculosis-specific CD4 T Cells during
642 SIV/M. tuberculosis Coinfection. J Immunol **190:**6320-6328.
643 41. **Feldmesser M, Casadevall A, Kress Y, Spira G, Orlofsky A.** 1997. Eosinophil-
644 *Cryptococcus neoformans* interactions in vivo and in vitro. Infect Immun
645 **65:**1899-1907.
646 42. **Garro AP, Chiapello LS, Baronetti JL, Masih DT.** 2011. Eosinophils elicit
647 proliferation of naive and fungal-specific cells in vivo so enhancing a T helper
648 type 1 cytokine profile in favour of a protective immune response against
649 *Cryptococcus neoformans* infection. Immunology **134:**198-213.
650 43. **Garro AP, Chiapello LS, Baronetti JL, Masih DT.** 2010. Rat eosinophils
651 stimulate the expansion of *Cryptococcus neoformans*-specific CD4(+) and
652 CD8(+) T cells with a T-helper 1 profile. Immunology.

Downloaded from http://iai.asm.org/ on November 28, 2020 by guest

44. **Piehler D, Stenzel W, Grahnert A, Held J, Richter L, Kohler G, Richter T, Eschke M, Alber G, Muller U.** 2011. Eosinophils contribute to IL-4 production and shape the T-helper cytokine profile and inflammatory response in pulmonary cryptococcosis. Am J Pathol **179:**733-744.

45. **Linch SN, Kelly AM, Danielson ET, Pero R, Lee JJ, Gold JA.** 2009. Mouse eosinophils possess potent antibacterial properties in vivo. Infect Immun **77:**4976-4982.

46. **Erpenbeck VJ, Ziegert M, Cavalet-Blanco D, Martin C, Baelder R, Glaab T, Braun A, Steinhilber W, Luettig B, Uhlig S, Hoymann HG, Krug N, Hohlfeld JM.** 2006. Surfactant protein D inhibits early airway response in *Aspergillus fumigatus*-sensitized mice. Clin Exp Allergy **36:**930-940.

47. **Gardai SJ, Xiao YQ, Dickinson M, Nick JA, Voelker DR, Greene KE, Henson PM.** 2003. By binding SIRPalpha or calreticulin/CD91, lung collectins act as dual function surveillance molecules to suppress or enhance inflammation. Cell **115:**13-23.

48. **Atochina-Vasserman EN, Winkler C, Abramova H, Schaumann F, Krug N, Gow AJ, Beers MF, Hohlfeld JM.** 2011. Segmental allergen challenge alters multimeric structure and function of surfactant protein D in humans. Am J Respir Crit Care Med **183:**856-864.

49. **von Bredow C, Hartl D, Schmid K, Schabaz F, Brack E, Reinhardt D, Griese M.** 2006. Surfactant protein D regulates chemotaxis and degranulation of human eosinophils. Clin Exp Allergy **36:**1566-1574.

IAI Accepts published online ahead of print

Downloaded from http://iai.asm.org/ on November 28, 2020 by guest

IAI Accepts published online ahead of print

676

Downloaded from http://iai.asm.org/ on November 28, 2020 by guest

IAI Accepts published online ahead of print

677 **Figure Legends**

678

679 **Figure 1.** SP-D$^{-/-}$ mice are more resistant than WT mice to aerosol exposure of *C.*
680 *neoformans*. (A) Mice were exposed to aerosolized H99 Stud in full-body Madison
681 chambers and fungal burden was assessed in the lung up to 21 days post-infection. Each
682 time point was repeated at least twice for a total n of 7-8 mice/group. Representative
683 images from histological analyses of paraffin-embedded and H&E-stained lung tissue
684 from (B) WT mice, and (C) SP-D$^{-/-}$ mice after aerosol exposure. * $P < 0.05$, ** $P < 0.01$.

685

686 **Figure 2.** Total CD45^{+} cells are decreased in SP-D$^{-/-}$ mice compared to WT mice after *C.*
687 *neoformans* infection. Flow cytometric analysis of total CD45^{+} cells in WT and SP-D$^{-/-}$
688 mice after *C. neoformans* infection in (A) lung interstitium (Day 3: n = 5-9 mice/group;
689 Day 7: n = 14-21 mice/group), and (B) lung BAL (Day 3: n = 1-2 samples/group; Day 7:
690 n = 5-8 samples/group; samples were pooled and normalized to per mouse cell counts).
691 Shown in Panels A and B are absolute numbers of cells per mouse calculated from total
692 cellularity obtained and the percentage of CD45^{+} cells. Frequency of PMNs in lung
693 interstitium (C) and BAL (D), CD11c^{+}MHCII^{int} cells in lung interstitium (E) and BAL
694 (F), CD11c^{+}MHCII^{hi} cells in lung interstitium (G) and BAL (H), and lymphocytes / other
695 CD45^{+} cells in lung interstitium (I) and BAL (J). In Panels C-J, data are shown as
696 percentages of CD45^{+} cells. * $P < 0.05$ for WT infected vs. SP-D$^{-/-}$ infected mice
697 comparison.

698

Downloaded from http://iai.asm.org/ on November 28, 2020 by guest

IAI Accepts published online ahead of print

Figure 3. IL-5 production and eosinophil infiltration are reduced in infected SP-D$^{-/-}$ mice compared to WT mice. WT and SP-D$^{-/-}$ mice were infected intranasally with 5x10^5 H99 Stud cells. (A) Eosinophils in BAL were assessed seven days post-infection via cytospin and H&E staining (n = 3-11 mice/group). (B) IL-5 protein levels were measured three days post-infection in BAL fluid by ELISA (n = 8-10 mice/group). (C) IL-5 mRNA steady-state level was measured on days 1-3 post-infection in post-lavaged lung tissue (n = 4-10 mice/group). (D) Mice were administered IL-5 neutralizing antibodies at the time of infection. Eosinophils were assessed in BAL seven days post-infection via cytospin and H&E staining. For the IL-5 blockade, data are shown as frequency of the respective isotype-treated control (n = 12-14 mice/group). * $P < 0.05$, ** $P < 0.01$, *** $P < 0.001$. Photomicrographs show representative cytospins used for analysis of: (E) saline-treated WT mice, (F) saline-treated SP-D$^{-/-}$ mice, (G) *C. neoformans*-infected WT mice, and (H) *C. neoformans*-infected SP-D$^{-/-}$ mice. Arrowheads indicate macrophages and arrows indicate eosinophils.

Figure 4. IL-5 overexpressing mice are more susceptible to *C. neoformans* than WT mice. (A) Pulmonary fungal burden at seven days post-*C. neoformans* infection in WT and IL-5Tg. *** $P < 0.001$. (B) Survival analysis of WT and IL-5Tg mice (two independent experiments for a total n of at least 18 mice/group; $P < 0.0001$).

Downloaded from http://iai.asm.org/ on November 28, 2020 by guest

IAI Accepts published online ahead of print

721 **Figure 5.** IL-5 overexpression increases the susceptibility of SP-D$^{-/-}$ mice to *C.*
722 *neoformans*. (A) Pulmonary fungal burden at fourteen days post-*C. neoformans* infection
723 in WT, IL-5Tg, SP-D$^{-/-}$, and IL-5TgxSP-D$^{-/-}$ mice. * $P < 0.05$, ** $P < 0.01$, *** $P < 0.001$.
724 (B) Survival analysis of WT, IL-5Tg, SP-D$^{-/-}$, and IL-5TgxSP-D$^{-/-}$ mice (two independent
725 experiments for a total n of at least 3 mice/group; P values: WT vs. SP-D$^{-/-}$ < 0.001; WT
726 vs. IL-5TgxSP-D$^{-/-}$ = NS; IL-5TgxSP-D$^{-/-}$ vs. SP-D$^{-/-}$ < 0.05; and IL-5TgxSP-D$^{-/-}$ vs. IL-
727 5Tg < 0.001.)
728
729 **Figure 6.** Representative photomicrographs from H&E-stained lung sections seven days
730 after *C. neoformans* infection: (A) WT sham-infected mice, (B) WT *C. neoformans*-
731 infected mice, (C) SP-D$^{-/-}$ sham-infected mice, (D) SP-D$^{-/-}$ *C. neoformans*-infected mice,
732 (E) IL-5Tg sham-infected mice, (F) IL-5Tg *C. neoformans*-infected mice, (G) IL-
733 5TgxSP-D$^{-/-}$ sham-infected mice, and (H) IL-5TgxSP-D$^{-/-}$ *C. neoformans*-infected mice.
734 Arrows indicated *C. neoformans* cells; the cell wall of *C. neoformans* is stained by
735 hematoxylin.
736

Downloaded from http://iai.asm.org/ on November 28, 2020 by guest

IAI Accepts published online ahead of print

Tables

TABLE 1: Histological analysis of H&E-stained lung sections 21 days post-aerosol challenge.[a,b]

Genotype	Necro-sis	Hemor-rhage	Edema	*Crypto-coccus*	Inflam-mation	Composite
WT	2.7	1.3	1	7.7	6.7	19.3
SP-D$^{-/-}$	3	1.7	0.3	3.7	4	12.7

[a] Data are expressed as means; N = 2-5 mice/group.
[b] Sham-infected WT and SP-D$^{-/-}$ mice received a score of 0 for each category.

TABLE 2: Levels of BAL cytokines and chemokines (pg/mL) 7 days post-infection[a]

Cytokine	WT Control	SP-D$^{-/-}$ Control	WT Infected	SP-D$^{-/-}$ Infected	WT Fold Change	SP-D$^{-/-}$ Fold Change
IFN-γ	9.2(0.1)	12(2)	50(10)[b]	49(8)[b]	6.0[e]	4.2
TNF-α	10.1(0.5)	10.1(0.5)	20(3)[b]	16(2)[b,c]	2.0	1.6
IL-4	16.2(0.3)	16.1(0.3)	110(20)[b]	160(20)[b]	7.0	9.8
IL-5	9.3(0.07)	9.3(0.07)	310(40)[b]	550(70)[b,c]	33.8[e]	59.2
IL-6	14(1)	14(1)	130(20)[b]	200(30)[b]	9.4	13.9
IL-12	9(2)	40(8)[d]	60(8)[b]	81(7)[b]	6.7[e]	2.0
IL-13	17(2)	17(2)	800(80)[b]	800(200)[b]	47.1[e]	49.1
IL-17	5(1)	5(1)	7.4(0.6)	9(1)[b]	1.4	1.6
IP-10	8(2)	7(2)	57(6)[b]	140(10)[b,c]	7.3[e]	18.8
MCP-1	19(2)	24(5)	300(30)[b]	530(50)[b,c]	16.0	22.2
MIG	5(2)	7(3)	29(6)	42(9)[b]	5.5	6.4
MIP-1α	27(8)	29(7)	120(20)	190(40)[b]	4.6	6.7
VEGF	90(10)	160(10)[d]	30(8)[b]	50(20)[b]	0.4	0.3
FGF basic	40(9)	90(20)	100(20)	170(30)	2.5	1.9
KC	180(60)	230(50)	94(5)	130(40)	0.6	0.6

[a] Concentrations are expressed as Mean(SE); N = 10-15 mice/group; data accumulated from 3-4 independent experiments.
[b] Infected mice are significantly different than respective saline-treated control mice.
[c] Infected SP-D$^{-/-}$ are significantly different than infected WT mice.
[d] Baseline SP-D$^{-/-}$ mice are significantly different than baseline WT mice.
[e] Fold change is significantly different in WT and SP-D$^{-/-}$ mice.

Downloaded from http://iai.asm.org/ on November 28, 2020 by guest

IAI Accepts published online ahead of print

TABLE 3: Histological analysis of H&E-stained lung sections 7 days post-infection[a,b]

Genotype	Necro-sis	Hemor-rhage	Edema	*Crypto-coccus*	Inflam-mation	Composite
WT	2.3	1.3	0.8	4.3	4.0	12.8
SP-D$^{-/-}$	1.4	1.0	0.0	3.6	2.6	8.6
IL-5Tg	3.3	2.3	1.6	6.5	5.8	19.4
IL-5Tg x SP-D$^{-/-}$	1.7	1.0	0.7	3.0	3.0	9.3

[a] Data are expressed as means; N = 2-5 mice/group.

[b] All sham-infected mice received a score of 0 for each category except IL-5Tg mice, which received a mean score of 0.3 for inflammation and IL-5TgxSP-D$^{-/-}$ mice, which received a mean score of 0.5 for hemorrhage and 1 for inflammation.

Downloaded from http://iai.asm.org/ on November 28, 2020 by guest

IAI Accepts published online ahead of print

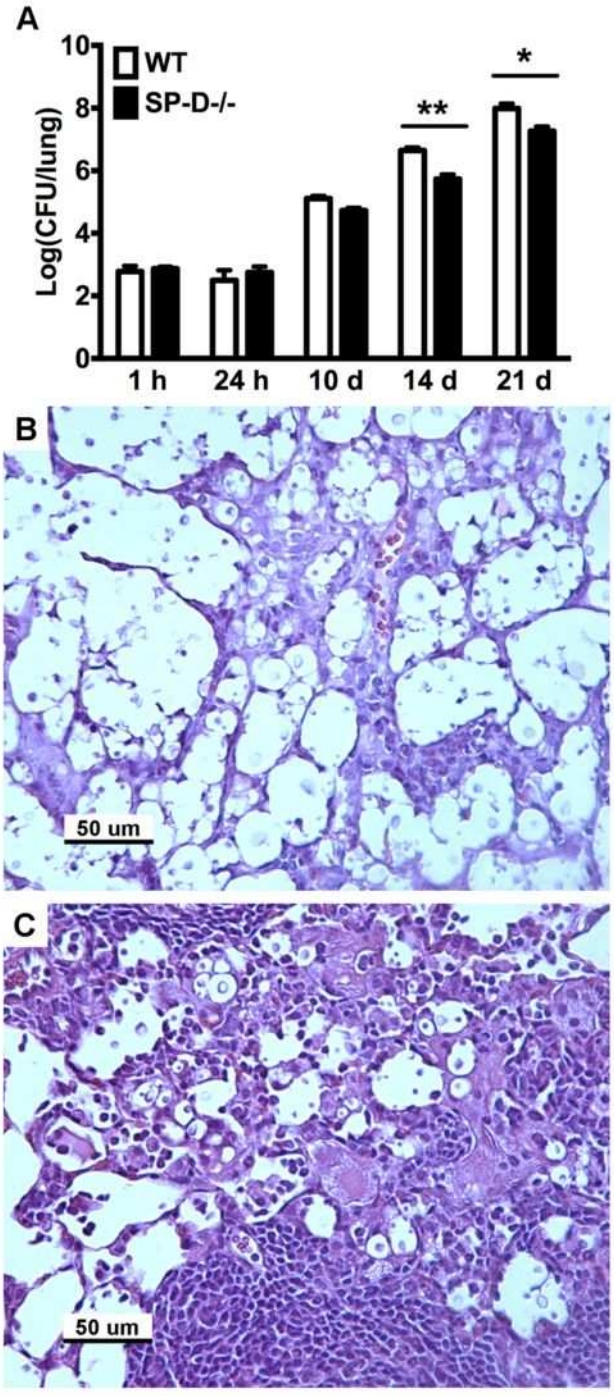

Downloaded from http://iai.asm.org/ on November 28, 2020 by guest

IAI Accepts published online ahead of print

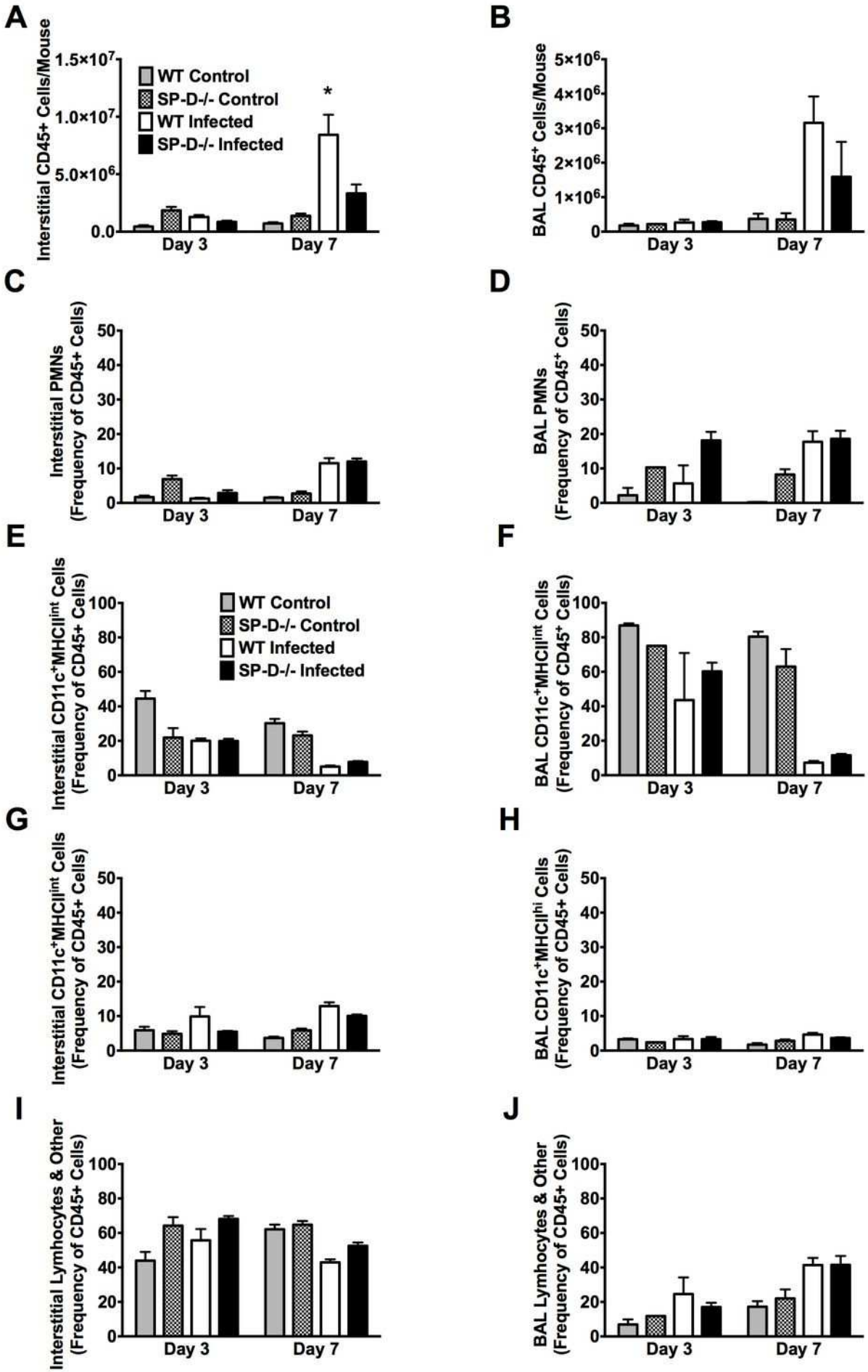

Downloaded from http://iai.asm.org/ on November 28, 2020 by guest

IAI Accepts published online ahead of print

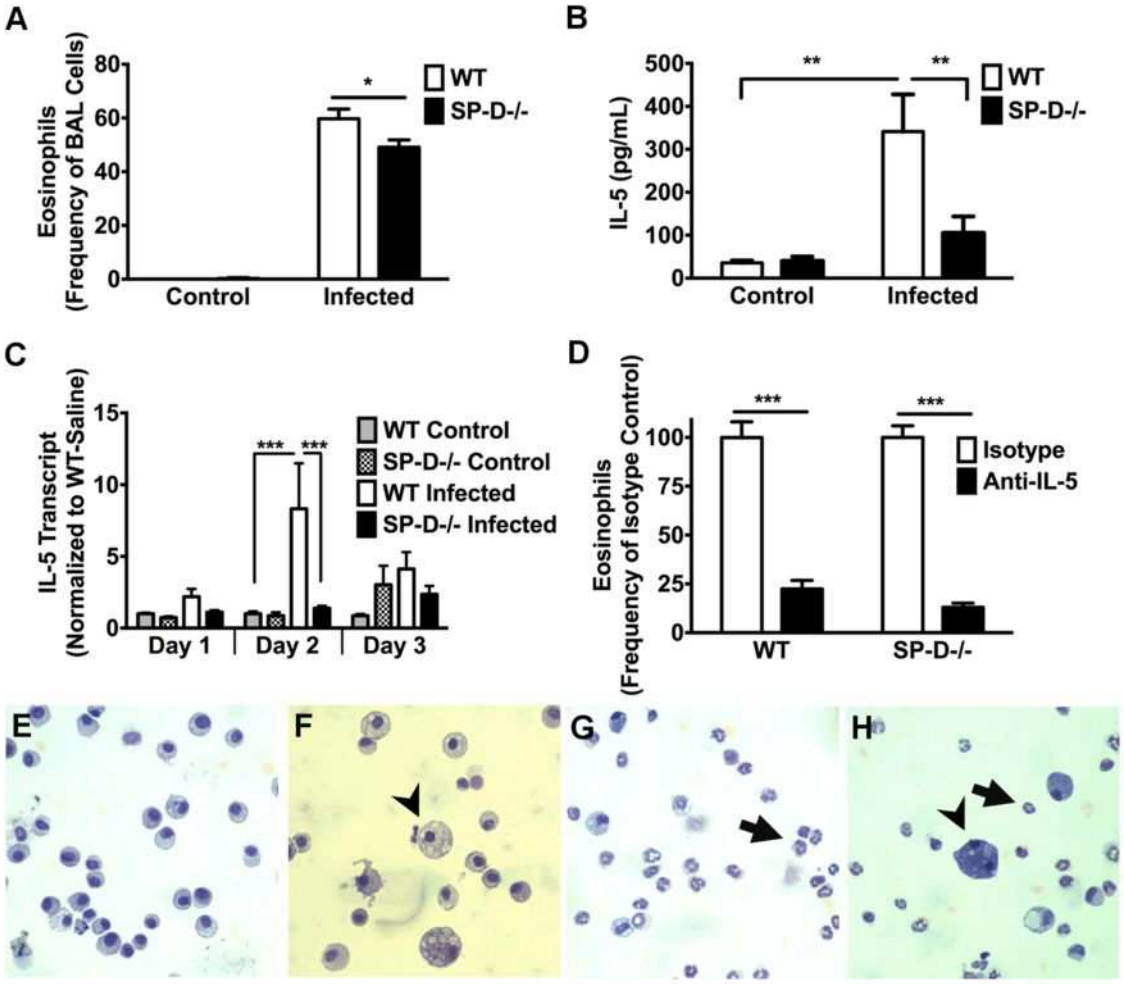

Downloaded from http://iai.asm.org/ on November 28, 2020 by guest

IAI Accepts published online ahead of print

Downloaded from http://iai.asm.org/ on November 28, 2020 by guest

IAI Accepts published online ahead of print

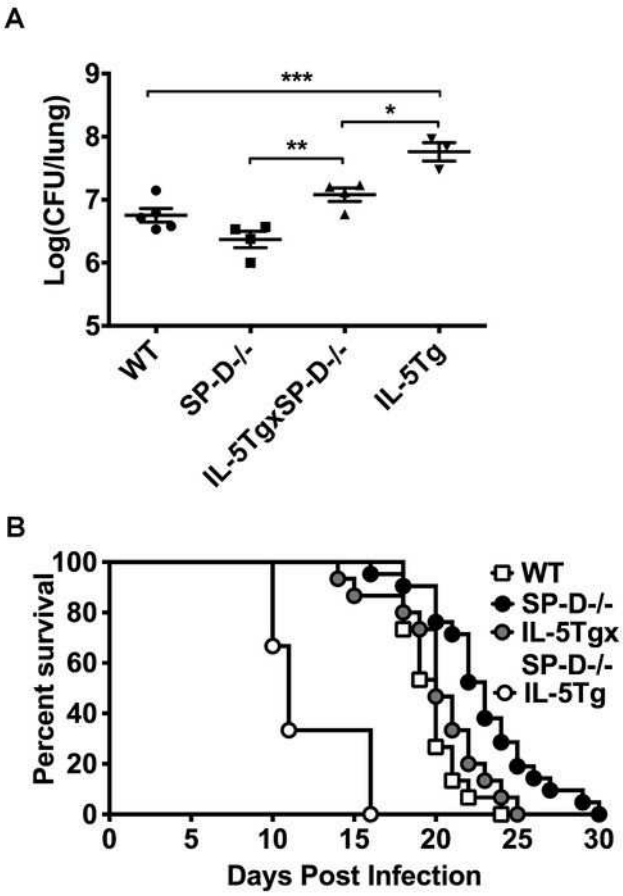

Downloaded from http://iai.asm.org/ on November 28, 2020 by guest

IAI Accepts published online ahead of print

Downloaded from http://iai.asm.org/ on November 28, 2020 by guest